Compact Design of Wide Bandpass, Symmetric and Asymmetric Dual Bandpass Filters with Finline and Split Ring Resonators

V. Madhusudana Rao [1] and B. Prabhakara Rao [2]

[1] Department of Electronics and Communication Engineering
Jawaharlal Technological University, Kakinada, INDIA-532003
vepakayala@gmail.com

[2] Rector of Jawaharlal Nehru Technological University, Kakinada, INDIA-532003
drbpr@rediffmail.com

Abstract ─ The finline based transmission line is used for realization of wide band pass filter. In this paper designing a bandpass filter for wide bandwidth, based on parallel coupled unilateral three finline structures. A design graph for symmetric three unilateral finline structures is presented for the design of bandpass filter. A bandpass filter of order 3 having center frequency of 10 GHz with fractional bandwidth of 20% is designed fabricated and measured. This wide bandpass filter is converted into symmetric and asymmetric dual band pass filters with the help of metamaterials (Split Ring Resonators SRR) on the other side of the finline structure is simulated with High Frequency Structure Simulator (HFSS) and fabricated. Transmission (S_{21}) and reflection (S_{11}) parameters of measured results compared with simulated results.

Index Terms ─ Asymmetric dual bandpass filters, metamaterials, split ring resonator (SRR), unilateral finline, wide band pass filter.

I. INTRODUCTION

The metamaterials or artificial electromagnetic (EM) materials are those materials that do not have any natural occurrence in nature. They are synthesized artificially through man-made processes. Their structures exhibit strange and uncommon electromagnetic properties. Metamaterial is a material which gains its properties from its structure rather than directly from its composition. These materials are often recorded as left handed materials or double negative materials as they have simultaneous negative permittivity ($\varepsilon < 0$) and permeability ($\mu < 0$). Due to the fact that both ε and μ are negative, these materials show negative index of refraction. In 1968, Victor Veselago studied and theoretically suggested these materials [1]. As the name suggests, left-handed materials obey left hand rule which is in complete contrast to the right-hand rule followed for usual materials. The electric field, magnetic field and wave vector of electromagnetic wave propagation in left-handed (LH) materials are opposite to those in right-handed materials. It has also been demonstrated that many other resonator topologies, derived from the basic SRR proposed by Pendry *et al.* [2], are appropriate to achieve effective (continuous) media with negative permeability. With the rapid development of microwave and millimeter wave communication systems, it greatly stimulates the demand on high performance bandpass filters with compact dimensions, low insertion loss, high attenuation in stopband and low cost [3, 4]. The finline transmission line is a wave guiding structure which is increasingly used as millimeter wave component due to various advantages such as high transmission level, reducing size, and weight. The wide bandpass filter structure based on finline topology which offer the benefit to concentrate the fields near the slot of planner transmission line embedded in side a hallow wave guide to prevent any radiation losses [5, 6]. With the help of these SRRs, this wide bandpass filter has been converted into symmetric and asymmetric dual bandpass filters presented in this paper.

II. ANALYSIS OF THREE COUPLED UNILATERAL FINLINES

The dispersion characteristics of multiple coupled unilateral finlines on isotropic substrate have been evaluated by using full wave modal analysis as shown in Fig. 1. In this modal analysis, all the field components are constructed in terms of x-components of electric and magnetic fields in each region, which are expanded in terms of modal fields with unknown coefficients, are given below.

The Maxwell equation is:

$$\begin{bmatrix} E_t \\ H_t \end{bmatrix} = \frac{1}{\left(k_o^2 \varepsilon_r - k_x^2\right)} \begin{bmatrix} \partial/\partial x & j\omega\mu_o x \\ -j\omega\varepsilon_o\varepsilon_r x & \partial/\partial x \end{bmatrix} \begin{bmatrix} \nabla_t E_x \\ \nabla_t H_x \end{bmatrix}. \quad (1)$$

The x-component of the electric and magnetic fields

Submitted On: February 26, 2017
Accepted On: August 16, 2017

satisfy the Helmholtz equation:

$$\left[\frac{\partial^2}{\partial x^2}+\frac{\partial^2}{\partial y^2}+\left(k_o^2\varepsilon_r-\beta^2\right)\right]\begin{bmatrix}E_x\\H_x\end{bmatrix}=0. \quad (2)$$

Here side walls are considered to be electric walls. Solutions of the equations in the three regions are:

$$E_x^{(1)}=\sum_{n=1}^{\infty}A_{n1}Cos\left[\Gamma_{n1}(x-h_1)\right]Sin(\alpha_n y)e^{-j\beta z}, \quad (3)$$

$$H_x^{(1)}=\sum_{n=0}^{\infty}B_{n1}Sin\left[\Gamma_{n1}(x-h_1)\right]Cos(\alpha_n y)e^{-j\beta z}, \quad (4)$$

$$E_x^{(2)}=\sum_{n=1}^{\infty}\left[A_{n2}Sin(\Gamma_{n2}x)+A'_{n2}Cos(\Gamma_{n2}x)\right]Sin(\alpha_n y)e^{-j\beta z}, \quad (5)$$

$$H_x^{(2)}=\sum_{n=0}^{\infty}\left[B_{n2}Cos(\Gamma_{n2}x)+B'_{n2}Sin(\Gamma_{n2}x)\right]Cos(\alpha_n y)e^{-j\beta z}, \quad (6)$$

$$E_x^{(3)}=\sum_{n=1}^{\infty}A_{n3}Cos\left[\Gamma_{n3}(x+d+h2)\right]Sin(\alpha_n y)e^{-j\beta z}, \quad (7)$$

$$H_x^{(3)}=\sum_{n=0}^{\infty}B_{n3}Sin\left[\Gamma_{n3}(x+d+h2)\right]Cos(\alpha_n y)e^{-j\beta z}, \quad (8)$$

where k_0 is propagation constant, A_{n1}, B_{n1}, A_{n2}, B_{n2}, A'_{n2}, B'_{n2}, A_{n3} and B_{n3} are amplitude constants;

$$\Gamma_{n1}=\sqrt{k_0^2-\alpha_n^2-\beta^2},$$

$$\Gamma_{n2}=\sqrt{k_0^2\varepsilon_{r2}-\alpha_n^2-\beta^2},$$

$$\Gamma_{n3}=\sqrt{k_0^2\varepsilon_{r3}-\alpha_n^2-\beta^2},$$

$$\alpha_n=\frac{(2n+1)\pi}{b},\ \beta = 2\Pi/\text{wavelength}.$$

The boundary conditions at x = h1, (-h2+d) and y = ± b/2 have been incorporated. Using these boundary conditions in Eq. (1), the other field components (3)-(8) can be derived.

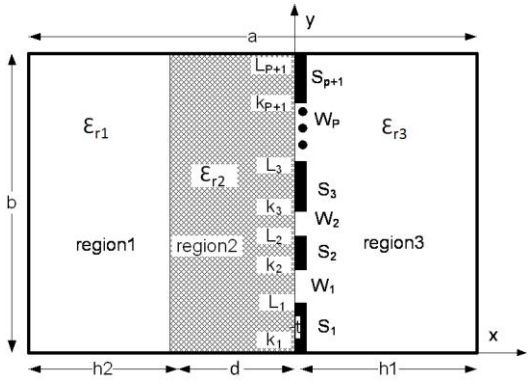

Fig. 1. Cross-section view of multiple edge coupled unilateral fin-line on isotropic substrate.

A. Normal mode parameters

The propagation constants are evaluated by applying the Galerkin's method to the transformed Green's function matrix relating the voltage and electric fields at various boundaries of the structure and solving for the roots of the determinant of the Eq. (1):

$$\sum_{k=1}^{\infty}c_k\sum_{n=0}^{\infty}p_nG_{11}L_{2n}^kL_{2n}^m+\sum_{k=1}^{\infty}d_k\sum_{n=0}^{\infty}q_nG_{12}L_{1n}^kL_{2n}^m=0.$$

$$\sum_{k=1}^{\infty}c_k\sum_{n=1}^{\infty}p_nG_{21}L_{2n}^kL_{1n}^m+\sum_{k=1}^{\infty}d_k\sum_{n=1}^{\infty}q_nG_{22}L_{1n}^kL_{1n}^m=0. \quad (9)$$

The set of basis functions used in this analysis are sinusoidal and expressed as follows:

$$V_z(y)=\frac{\cos\left[2(n-1)\pi\frac{(y-y_i)}{w_i}\right]}{\sqrt{1-\left[\frac{2(y-y_i)}{w_i}\right]^2}},\qquad V_y(y)=\frac{\sin\left[2n\pi\frac{(y-y_i)}{w_i}\right]}{\sqrt{1-\left[\frac{2(y-y_i)}{w_i}\right]^2}}, \quad (10)$$

where w_i being the width of the i^{th} fin, y_i is the distance from origin to the center of i^{th} fin.

B. Characteristics impedances

Mode characteristics impedance of the coupled unilateral finlines lines are evaluated for all hybrid modes in a straight forward manner by calculating the power associated with a given finline for a given mode. The finline mode impedance is given by:

$$Z_{lm}=\frac{(V_{lm})^2}{P_{lm}}, \quad (11)$$

where V_{lm} is the modal voltage of the l^{th} slot given by the integral of the electric field across the slot and P_{lm} is the partial modal power associated with the same slot when the m^{th} normal mode is excited.

III. FILTER DESIGNAND FABRICATION

The Fig. 2 shows the simulated structure of a resonator used to realize the wideband pass filter structure. The resonator consists of three parallel-coupled unilateral finlines approximately quarter wavelength long. In this paper multi resonators are cascaded to achieve high rejections. H field is perpendicular to the SRR plane (i.e., in the direction of X-axis) and the incident E field is in the same direction of the SRR rings (i.e., in the direction of Z-axis). The PEC type boundary conditions are applied at the boundary surfaces perpendicular to the E field, while the PMC type boundary conditions are applied at the boundary surfaces perpendicular to the H field. Remaining boundaries are defined as the input and output ports.

The six port impedance matrix parameters for a section of three coupled finlines of length *l* are found from mode characteristic impedances, phase velocities and voltage ratios [7-10]. This three-coupled finline

structure supports three dominant modes as OE, EE, and OO, which correspond to 1, 2 and 3, respectively. Each mode has its own modal phase constant, eigen voltage vector and characteristic impedance. The eigen voltage matrix for symmetrical three line which have equal fin-width and spacing are given by:

$$[\mathrm{Mv}] = \begin{bmatrix} 1 & 1 & 1 \\ \mathrm{m}_1 & 0 & \mathrm{m}_3 \\ 1 & -1 & 1 \end{bmatrix}.$$

Each vector of $[\mathrm{M_V}]$ is the eigen voltage vector of the matrix product [L] [C]. The matrix $[\mathrm{M_V}]$ can be used to derive the relation between port voltages and port currents:

$$\begin{bmatrix} V_A \\ V_B \end{bmatrix} = \begin{bmatrix} Z_A & Z_B \\ Z_B & Z_A \end{bmatrix} \begin{bmatrix} I_A \\ I_B \end{bmatrix}, \tag{12}$$

where

$$[V_A] = [V_1, V_2, V_3]^T,\ [V_B] = [V_4, V_5, V_6]^T,$$
$$[I_A] = [I_1, I_2, I_3]^T,\ [I_B] = [I_4, I_5, I_6]^T. \tag{13}$$

The impedance matrix $[Z_A]$ and $[Z_B]$ can be derived as:

$$[Z_A] = [M_V]\ \ diag[-jZ_{mi}\ cot\theta_i\ ][M_V]^T. \tag{14}$$

Now $\theta_i = \beta_i l$ with β_i is the phase constant of the i^{th} mode, l the length of the coupled section, and Z_{mi} given by:

$$Z_{mi} = \frac{Z_{oi}}{m_i^2 + 2}, \tag{15}$$

where Z_{oi} is the characteristic impedance of i^{th} mode. In Eq. (15), m_2=0. Comparing the two port Z-Parameters of the circuit in Fig. 3 (b) with Fig. 3 (c), we obtain Eqs. (16), (17), (18):

$$m_1 Z_{m1} - m_3 Z_{m3} = JZ_A Z_B, \tag{16}$$
$$m_1^2 Z_{m1} - m_3^2 Z_{m3} = Z_A(J^2 Z_A Z_B + 1), \tag{17}$$
$$Z_{m1} + Z_{m3} = Z_B(J^2 Z_A Z_B + 1), \tag{18}$$
$$m_1 Z_{m1} \approx \left[\frac{2+\mu^2}{2\mu}\right](Z_0/2)(J^2 Z_0^2 + JZ_0 + 1), \tag{19}$$
$$m_3 Z_{m3} \approx \left[\frac{2+\mu^2}{2\mu}\right](Z_0/2)(J^2 Z_0^2 - JZ_0 + 1), \tag{20}$$

where

$$\mu = \frac{\sqrt{2\left[2(Z_{ee}-Z_{oo})^2 - Z_{oe}(Z_{oe}-Z_{ee}-Z_{oo}) - Z_{ee}Z_{oo}\right]}}{2Z_{ee} - Z_{oe} - Z_{oo}}.$$

The value of JZ_O for each admittance inverter can be determined from the values of lumped circuit elements of the low pass prototype:

$$J_1 = \frac{1}{Z_0}\sqrt{\frac{\pi\Delta}{2g_1}}, \tag{21}$$
$$J_n = \frac{1}{Z_0}\sqrt{\frac{\pi\Delta}{2g_{n-1}g_n}},\ for\ n = 2, 3.....N, \tag{22}$$
$$J_{N+1} = \frac{1}{Z_0}\sqrt{\frac{\pi\Delta}{2g_N g_{N+1}}}, \tag{23}$$

where $\Delta = \frac{\omega_2 - \omega_1}{\omega_0}$.

For N = 3, characteristic impedance (Z_0) = 100 Ω, the values of g_1 to g_{N+1} are given below using [11]. g_1 = 1.5963, g_2 = 1.0967, g_3 = 1.5963, g_4 = 1.0000. Once JZ_O is known, the values of $m_1 Z_{m1}$ and $m_3 Z_{m3}$ for each coupled section can be known. The values of $m_1 Z_{m1}$ and $m_3 Z_{m3}$, for Section I are 82.02 Ω and 64.69 Ω respectively, and for the Section II are 37.65 Ω and 40.94 Ω respectively. The designed filter dimension has been simulated with HFSS. The optimized filter dimension has been shown in Table 1.

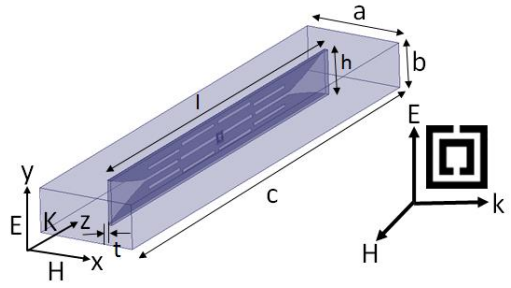

Fig. 2. Simulated structure of parallel coupled three finline wide bandpass filter housed in X-band wave guide (dimensions are a = 22.86 mm, b = 10.16 mm, c = 111 mm) and RT-Duriod 5880™ dielectric substrate parameters (dielectric constant (ε_r) = 2.2, substrate thickness (t) = 0.8 mm, length (l) = 90 mm, height (h) = 10.16 mm, loss tangent is 0.0009, frequency = 10 GHz).

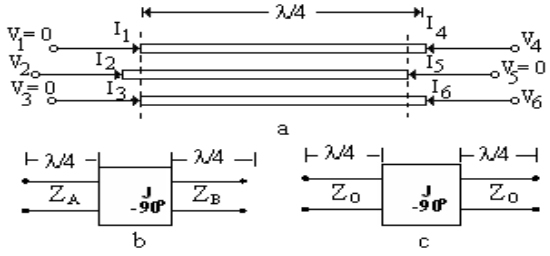

Fig. 3. Reduction of a coupled three-finline section to a two-port network: (a) coupled three-line section as a six-port network, (b) equivalent admittance inverter, and (c) further approximated admittance inverter.

Table 1: Three finline coupled wide bandpass filter (resonator parameters), dimensions are in mm

Dimensions	Designed Data		Optimized Data	
	Section 1	Section 2	Section 1	Section 2
W	0.650	0.68	0.750	0.750
S	1.320	2.370	1.400	2.400
L	9.592	10.164	12.970	13.413
G	1.975	2.033	1.076	1.633

The design graph of Fig. 4 for $\varepsilon_r = 2.2$ is used to determine the line width (W) and line spacing (S) of three coupled unilateral finlines at 10 GHz. Due to symmetry of filter, half part of the filter dimensions (width, spacing and length (L)) from center structure is designated in two sections have been mentioned in Table 1. With this data, the three coupled finline structure have been simulated with HFSS and fabricated. The pattern of the fabricated filter has been shown in Fig. 5.

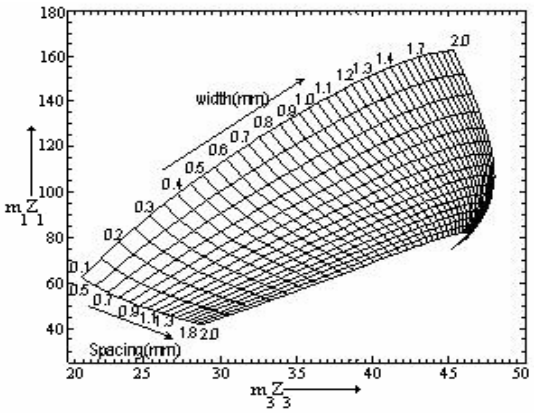

Fig. 4. The bandpass filter design graph for a symmetric three unilateral finline structure.

The return loss S11 and insertion loss S21 over the frequency band have been given in Fig. 6. The insertion loss in passband is 0.5 dB and return loss is less than -10 dB, and stop band attenuation is 20 dB at 11.5 GHz frequency. The transmission (S21), reflection (S11) coefficients of simulated and measured wide bandpass filter is compared and found reasonably matched. This wide bandpass filter has been converted into dual bandpass filters by using metamaterial (SRR) concept.

IV. METAMATERIAL (SRR) CONCEPT

Pendry et al. in 1999, proposed split-ring resonators (SRRs), which is a set of two concentric planar rings with splits in them at opposite ends as depicted in Fig. 4 (a), printed on a thin dielectric substrate (ε_r = 2.2) RT-Duriod 5880™.

The rings are made of nonmagnetic metal like copper and have a small gap between them. The splits in the rings cause the structure to support resonant wavelengths much larger than the diameter of the rings, which cannot occur in closed rings. Thus, SRRs that have a negative index of refraction are capable of high-frequency magnetic response. Below the resonant frequency the magnetic permeability of a SRR is positive, and above resonance frequency is negative. SRRs demonstrate a quasi-static resonance by virtue of the distributed capacitance between concentric rings and overall rings inductance. Topology of the SRR and its equivalent-circuit models has been depicted in Fig. 7. They act as LC resonators and their equivalent-circuit model as depicted in Fig. 7 (c). Where Co is the total capacitance between the rings, and Cs = Co/4 where Cs is the series capacitance of the upper and lower halves of the SRR. Now we introduced double SRR on the other side of substrate at center as shown in Fig. 7. This double SRR creates negative effective permeability μ_{eff} (ω) at desired frequency. It creates a notch at resonance frequency. This is the useful characteristics for converting the wideband filter in to dual bandpass filters. The notch can be controlled by number of SRR for desired frequency. With this technique we can create symmetric and asymmetric dual bandpass filters for different band widths [13-18].

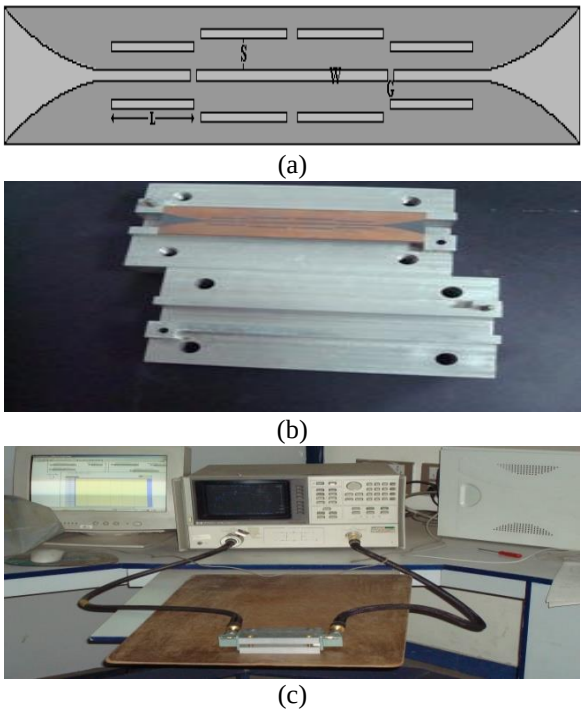

(a)

(b)

(c)

Fig. 5. (a) Simulated structure of parallel coupled three finline wide band pass filter of order 3, (where L = length of the resonators, S = spacing between resonators, W = width of resonators, G = gap between adjacent resonators). (b) Photo of X-band wave guide housing to keep this filter. (c) Photo of measurements setup of dual bandpass filters.

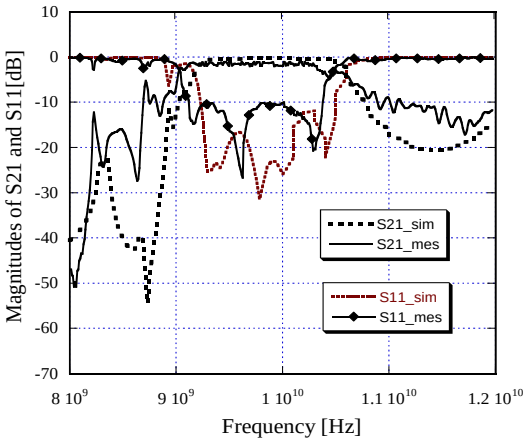

Fig. 6. Simulated and measured responses s-parameters of three finline wide bandpass filter.

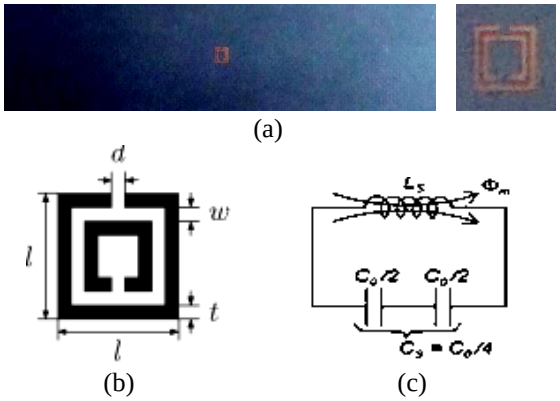

Fig. 7. (a) Photographic view of SRR fabricated on the back side of the substrate of three coupled finline wide bandpass filter and magnified view of this SRR besides this structure. (b) Copper SRR dimensions: l = 2.54 mm, t = 0.254 mm, w = 0.1252 mm, d = 0.254 mm, thickness = 0.038 mm and the conductivity = $5.8*10^7$ S/m. (c) Electrical equivalent circuit diagram of SRR.

Comparisons of measured and simulated S-parameters of asymmetric dual bandpass are shown in Fig. 8. We further simulated for different combinations of SRRs as shown in Table 2.

Table 2: Band width variations with number of SRRs

No of SRRs	Notch at Frequency
1 Cell	9.75 GHz
3 Cells	10.25 GHz
5 Cells	10.75 GHz
7 Cells	11.25 GHz
9 Cell	11.75 GHz

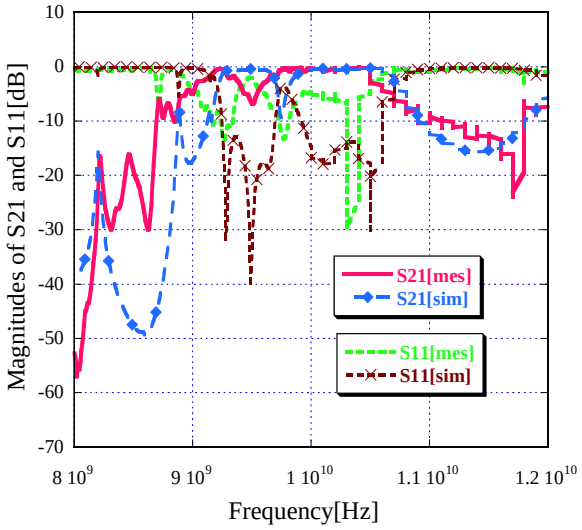

Fig. 8. Comparison plot of simulated and measured S-parameters of asymmetric dual bandpass filter.

V. CONCLUSION

This paper presents, asymmetric and symmetric dual bandpass filters that can be realized with these SRR in three coupled finline structure, to meet the transmission for particular frequency band which is possible for non-continuous channel. Modern communication transceivers require high performance microwave filters with low insertion loss, high frequency selectivity and small group delay variations. Most of the above said parameters will be obtained with these filters. Some of the most important advantages of these filters can be widely used in microwave and millimeter wave applications, exclusively in radar and satellite applications. These results have been compared with existing publications as shown in Table 3.

Table 3: Comparison with other proposed dual band-pass filters

Parameters	Ref. [17]	Ref. [18]	Ref. [13]	Proposed
Substrate	Roger 588 oLZ	Roger O3003	RT-Duriod	RT-Duriod
ε_r	1.96	3	10.2	2.2
1st and 2nd pass band frequencies [GHz]	4.1, 5.6	5.8, 8.7	0.9, 2.4	9.5, 10.3
Return loss S11 [dB]	<-15	<-22	<-15	<-15
Insertion loss S21 [dB]	<-0.1	<-2	<-2	<-0.5

REFERENCES

[1] V. G. Veselago, "The electrodynamics of substances with simultaneously negative values of permittivity and permeability," *Sov. Phys. USPEKHI*, vol. 10, p. 509, 1968.

[2] J. B. Pendry, A. J. Holden, D. J. Robbins, and W. J. Stewart, "Magnetism from conductors and enhanced nonlinear phenomena," *IEEE Trans. Microwave Theory Tech*., vol. 47, p. 2075, 1999.

[3] R. Marques, J. Martel, F. Mesa, and F. Medina, "Left handed–media simulation and transmission of EM waves in subwavelength split ring resonators-loaded metallic saveguides," *Physical Review Letters*, vol. 89, no. 18, Oct. 2002.

[4] R. W. Zoilkowski, "Design, fabrication, and testing of double negative metamaterials," *IEEE Trans. Antennas Propagate.*, vol. 51, no. 7, July 2003.

[5] B. Bhat and S. K. Koul, *Analysis, Design and Application of Finlines*. Artech House, 1987.

[6] P. J. Meier, "Integrated finline millimeter components," *IEEE Trans. Microwave Theory & Tech*., vol. MTT-22, no. 12, pp. 1209-1216, Dec. 1974.

[7] D. M. Syahkal and J. B. Davies, "An accurate, unified solution to various finline structures, of phase constant, characteristic impedance and attenuation," *IEEE Trans. Microwave Theory & Tech*., vol. MTT-30, no. 11, pp. 1854-1861, Nov. 1982.

[8] S. Luo, A. Biswas, and V. K. Tripathi, "Finline multiport couplers," *IEEE Trans. Microwave Theory & Tech*., vol. MTT-42, no. 12, pp. 2208-2215, Dec. 1994.

[9] A. Biswas and V. K. Tripathi, "Analysis and design of symmetric and multiple coupled finline couplers and filters," *in IEEE MTT-S Int. Microwave Symp. Dig*., pp. 403-406, 1990.

[10] J.-T. Kuo and E. Shih, "Wideband band-pass filter design with three line microstrip structures," *in IEEE MTT-S Int. Microwave Symp. Dig.*, pp. 1593-1596, 2001.

[11] D. M. Pozar, *Microwave Engineering*. John Wiley & Sons, Inc.

[12] T. Decoopman, A. Marteau, E. Lheurette, O. Vanbésien, and D. Lippens, "Left-handed electromagnetic properties of split-ring resonator and wire loaded transmission line in a fin-line technology," *IEEE Transactions on Microwave Theory and Techniques*, vol. 54, no. 4, Apr. 2006.

[13] G. Jang and S. Kahng, "Design of a dual-band metamaterial bandpass filters using Zeroth order resonance," *Progress In Electromagnetics Research C*, vol. 12, pp. 49-162, 2010.

[14] S. Chaimool and P. Akkaraekthalin, "Miniaturized wideband bandpass filter with wide stopband using metamaterial based resonator and defected ground structure," *Radio Engineering*, vol. 21, no. 2, June 2012.

[15] X. Q Lin, J. Y. Jin, Y. Jiang, and Y. Fan, "Metamaterial-inspired waveguide filters with compact size and sharp skirt selectivity," *Journal of Electromagnetic Waves and Applications*, vol. 27, no. 2, pp. 224-232, 2013.

[16] N. Benmostefa, M. Meliani, and H. Ouslimani, "Metamaterial tunable filter design," *Journal of Electromagnetic Analysis and Applications*, no. 5, pp. 250-254, June 2013.

[17] M. Duran Sindreu, J. Bonache, F. Martin, and T. Itoh, "Single–layer fully-planar extended-composite right-/left handed transmission lines based on substrate integrated waveguides for dual-band and quad- band applications," *International Journal of Microwave and Wireless Technologies*, vol. 3, no. 5, pp. 213-220, May 2013.

[18] A. Boubraki, F. Choubani, T. H. Vuong, and J. David, "A compact dual band band pass filter using a new topology of transmission line metamaterial," *PIERS Proceeding*, Guangzhou, China, Aug. 25-28, 2014.